Journal of Superconductivity and Novel Magnetism
https://doi.org/10.1007/s10948-017-4452-3

ORIGINAL PAPER

Surface Effects on the Dynamic Behavior of Vortices in Type II Superconducting Strips with Periodic and Conformal Pinning Arrays

N. P. Vizarim[1] · M. Carlone[1] · L. G. Verga[2] · P. A. Venegas[3]

Received: 6 November 2017 / Accepted: 17 November 2017

Abstract

Using molecular dynamics techniques, we simulate the vortex behavior in a type II superconducting strip in the presence of triangular and two types of conformal pinning arrays, one with a pinning gradient perpendicular to the driving force (C1) and the other parallel (C2), at zero temperature. A transport force is applied in the infinite direction of the strip, and the magnetic field is increased until the rate between the density of vortices (n_v) and pinning (n_p) reaches $n_v/n_p = 1.5$. Our results show a monotonic increase, by steps, of the vortex density with the applied magnetic field. Besides, each pinning lattice presents a different vortex penetration delay. For the triangular pinning array, different than the case of infinite films, here the system exhibits only one pronounced depinning force peak at $n_v/n_p = 1$. However, the depinning force peak is present for only one value of field, in the range of fields where $n_v/n_p = 1$ is stable. For the case of conformal pinning arrays, in analogy to what is observed in infinite films, no commensurability depinning force peaks were found. In the present case, the C1 array is more efficient at low fields, all arrays are equivalent in the intermediate fields, and the C2 array is more efficient for high fields. We also show that for the C1 array at high fields, vortices depin following the conformal arches, from the edge to the center. For the C2 array, the depinning force is higher when compared to that of C1, because this particular conformal structure prevents the formation of easy vortex flow channels.

Keywords Superconductivity · Vortex dynamics · Surface effects · Conformal pinning · Periodic pinning

1 Introduction

Superconductors have attracted much attention from the scientific community, since one of its main characteristics is to flow a transport current without energy dissipation. However, when type II superconducting films are submitted to an external magnetic field, quantized flux lines penetrate the material characterizing the mixed state. Inside the material, these vortices arrange themselves in a hexagonal (or triangular) lattice, known as the Abrikosov lattice [1]. When a transport current density is applied, vortices move through the material due to the Lorentz force, dissipating energy and destroying the zero-resistance state [2], which is not useful for technological applications [3]. Fortunately, it had been discovered that defects inside the superconductor could work as pinning centers, avoiding the vortex motion and consequently the energy dissipation [4]. Since then, several authors began to investigate pinning mechanisms in type II superconductors [5–15].

Several works had investigated the effects of periodic [12–40], quasi-periodic [41–48], and randomly distributed [49–54] pinning centers in superconducting films. For periodic pinning, such as square [12–21], triangular [30–35, 55], honeycomb [27, 29, 30, 38], and Kagomé [27–29, 32, 37], vortices tend to match the pinning lattice in commensurate patterns, which greatly enhances the

✉ N. P. Vizarim
nicolas.vizarim@fc.unesp.br

[1] POSMAT—Programa de Pós-Graduação em Ciência e Tecnologia de Materiais, Faculdade de Ciências, Universidade Estadual Paulista—UNESP, Bauru, SP, CP 473, 17033-360, Brazil

[2] Department of Chemistry, University of Southampton, Highfield, Southampton SO17 1BJ, UK

[3] Departamento de Física, Faculdade de Ciências, Universidade Estadual Paulista—UNESP, Bauru, SP, CP 473, 17033-360, Brazil

Published online: 28 November 2017

critical current density. However, these enhancements occur at specific values of magnetic fields, resulting in high oscillations of the critical current as a function of the applied field [13, 14, 29, 33–40]. On the other hand, quasi-periodic arrays, such as Penrose [43, 44, 48], hyperbolic tessellations [47], and Archimedean tilings [41, 46], show unusual commensurability effects for several values of applied magnetic fields; besides that, for a wide range of fields, the critical depinning currents are high. Recently, Ray et al. [56] proposed conformal pinning arrays created by a conformal angle-preserving transformation of a regular pinning array. As a result, they demonstrated that the conformal crystal strongly enhances the vortex pinning due to the gradient of defects associated with the sixfold symmetry of the lattice that the transformation preserves. Moreover, it was shown that the conformal lattice presents high values of critical depinning currents for a much wider range of applied magnetic fields [56, 57]. Since then, conformal crystals have been investigated both theoretically [58–61] and experimentally [62, 63] for their unique features.

Nowadays, there is a great technological interest in superconducting devices with reduced dimensions. In these cases, the size effects play an important role. With this purpose, several authors investigated theoretically finite and semi-finite size systems with diverse geometries, using the Ginzburg-Landau [64–75] and London approach [76–80]. However, there are still open questions about critical depinning currents and vortex behavior in such systems, specially under the influence of pinning arrays.

In samples where the width is comparable to the London penetration depth, the Bean-Livingston surface barrier effects [81] must be taken into account. In the theoretical description of the system, the boundary conditions of the surface are described by two interactions: the interaction between the vortices and the shielding currents, which is repulsive, and the interaction between vortices and their images outside the sample, which is attractive [81]. The competition between these two interactions satisfies the boundary conditions of the surface.

For the particular case of superconducting strips, some works had been conducted investigating vortex states, critical currents, and magnetization curves [76–79, 82–90]. In strips, vortices arrange themselves in chains of straight vortex lines due to the geometrical constraint [76], and the magnetization curves present several peaks, indicating the vortex lattice transitions with formation or destruction of the vortex chains [78, 88]. However, there are only few works investigating vortex dynamics under the influence of pinning centers in strips [72, 77, 86].

In this work, we numerically study the critical depinning forces of vortices under the influence of a triangular pinning lattice and two kinds of conformal pinning arrays as shown in Fig. 1 (which we refer to as C1 and C2) in type II superconducting strips. Using Langevin dynamics, we perform the calculations for values of the applied magnetic field until the rate between the density of vortices and pinning (n_v/n_p) reaches the value of 1.5, for all pinning landscapes and zero temperature. We show the effects of the surface barrier and pinning in the critical depinning forces, vortex trajectories, and dynamical phases and compare to infinite films. It is necessary to point out that, as we are working with very narrow strips, we do not expect to see flux avalanches [91, 92].

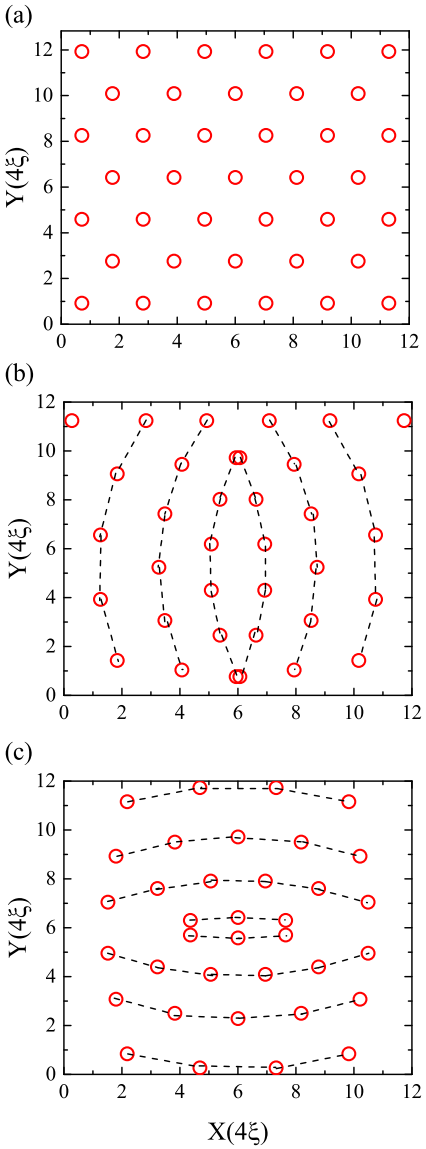

Fig. 1 Pinning site locations for the **a** regular triangular array, **b** conformal array 1 (C1), and **c** conformal array 2 (C2), where the open circles represent the pinning centers. The dashed lines are guides to the eye to see the arches of the conformal structure. The applied transport force is always in the y direction in this work, and the lengths x and y are in units of 4ξ

2 Model

We consider a type II superconducting strip in the xy plane, infinite along the y direction. The external magnetic field is applied perpendicular to the strip surface and zero temperature [76, 78]. Considering vortices as particles, their dynamical properties can be modeled using a set of Langevin equations:

$$\eta\frac{d\vec{r}_i(t)}{dt} = \sum\nolimits_{j\neq i}\nabla_i U_{vv}(r_{ij}) - \sum\nolimits_p \nabla_i U_p(r_{ip}) + \nabla_i U_H(r_i) + \nabla_i U_S(r_i) + \vec{F}_J \quad (1)$$

The left term of the equation represents the drag force, where the velocity of the vortex i is multiplied by the Bardeen-Stephen [93] friction $\eta = \Phi_0 H_{c2}/c^2\rho_n$. We modeled the interactions inside the strip following Carneiro [76], where the first term on the right side is the vortex-vortex interaction, described as

$$U_{vv}(r_{ij}) = \frac{C_v}{2}\sum_{kij}\ln\left\{\frac{\cosh\left[\frac{\pi(kL_y+y_i-y_j)}{L_x}\right]-\cos\left[\frac{\pi(x_i+x_j)}{L_x}\right]}{\cosh\left[\frac{\pi(kL_y+y_i-y_j)}{L_x}\right]-\cos\left[\frac{\pi(x_i-x_j)}{L_x}\right]}\right\} \quad (2)$$

The second term on the right is the vortex-pinning interaction, which is described as a Gaussian function [32, 33, 37, 54, 77]:

$$U_p(r_{ip}) = C_p e^{-(r_{ip}/a_p)^2} \quad (3)$$

The third term is the energy related to the vortex interaction with the screening Meissner supercurrents:

$$U_H(r) = \frac{C_v 4\pi\lambda^2 H}{\Phi_0}\sum\nolimits_i\left\{\frac{\cosh\left[\frac{(x_i-L_x/2)}{\lambda}\right]}{\cosh\left[\frac{L_x}{2\lambda}\right]} - 1\right\} \quad (4)$$

The fourth term is the potential energy given by the interaction of vortices with their self-images, which represents the anti-vortices outside the strip included by Bean and Livingston [81] to satisfy the boundary condition at the surface:

$$U_s(r) = \frac{C_v}{2}\sum\nolimits_i\ln\left\{\frac{4\text{sen}^2\left[\frac{\pi x_i}{L_x}\right]+\left(\frac{\pi\xi}{L_x}\right)^2}{\left(\frac{\pi\xi}{L_x}\right)^2}\right\} \quad (5)$$

where the constant C_v is the vortex strength given by $Cv = [\phi_0/(4^*\pi^*\lambda)]^2$; C_p is the pinning strength, settled as $C_p = 0.2C_v$; $a_p = \xi$ is the pinning range; H is the applied magnetic field; $L_x = 0.48\lambda$ is the strip width; L_y is the length of the simulation box, where the periodic boundary conditions are applied to simulate its infinite behavior; $r_{ij} = |r_j = r_i|$ is the distance between vortex i and vortex j; and $r_{ip} = |r_p - r_i|$ is the distance between vortex i and pinning center p. The Ginzburg-Landau parameter used is $\kappa = 100$. The length scales are normalized by 4ξ, the time scale by $\tau = 0.0016\eta\lambda^2/C_v$, the magnetic field by Φ_0/λ^2 , the energy scales by C_v, and the force scales by $25C_v/\lambda$, where ξ is the coherence length, λ is the London penetration depth, and Φ_0 is the flux quantum. The last term is the driving force due to the transport current $\vec{J}$:

$$\vec{F}_j = \left(\frac{\Phi_0}{c}\right)\vec{J}\times\hat{z} \quad (6)$$

We simulate the vortex behavior for several values of applied magnetic field up to $n_v/n_p = 1.5$, where n_v is the vortex density and n_p is the pinning density. In this work, we simulate the vortex behavior under the influence of three pinning arrays, illustrated in Fig. 1. For all cases in this work, we set $n_p = 156.25/\lambda^2$.

The vortex density and its correspondent vortex ground state were obtained using the generalized simulated annealing (GSA) method [94]. Then, the dynamical properties were simulated with a transport force applied in the infinite direction of the strip. This force started at $F = 0.0$ and was slowly increased in steps of $\Delta F = 0.002$ up to values as high as $F = 1.0$. For each value of F, we let 100,000 time steps for equilibration and 80,000 time steps for evaluation of the time averages. To determine the depinning forces, it is necessary to calculate the time average vortex velocity $V = \sqrt{V_x^2 + V_y^2}$, where $V_y = \langle V_y(t)\rangle = \langle\frac{1}{N_v}\sum_i\frac{dy_i}{dt}\rangle$ and $V_x = \langle V_x(t)\rangle = \langle\frac{1}{N_v}\sum_i\frac{dx_i}{dt}\rangle$. The average vortex velocity is proportional to the macroscopically measured voltage-current curve [15, 54]. The criterion used to determine the depinning forces is that $V < 0.001$ corresponds to vortex fluctuations around the equilibrium position [33, 37]. For the characterization

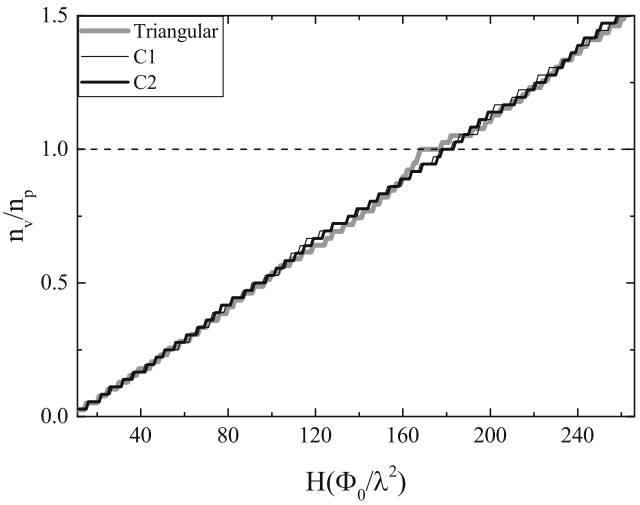

Fig. 2 The rate n_v/n_p as a function of the applied magnetic field H for all pinning distributions studied in this work. The horizontal dashed line indicates the first matching field line

of the different dynamic phases, we calculated the vortex trajectories, the time average vortex velocity, and vortex velocity derivative dV/dF, which is proportional to the differential resistance $dV/dF = \rho_f^{-1} dE/dJ$, where ρ_f is the flux flow resistivity [54].

3 Density as a Function of the Applied Magnetic Field and Vortex States

It is well known that in mesoscopic samples, the surface effect provokes a delay in the vortex penetration [76, 78, 84, 89, 90]. However, the presence of pinning centers, and the associated attractive interaction between them and the vortices, makes that the field necessary for the nucleation of a new vortex to be lower than in the absence of pinning [84].

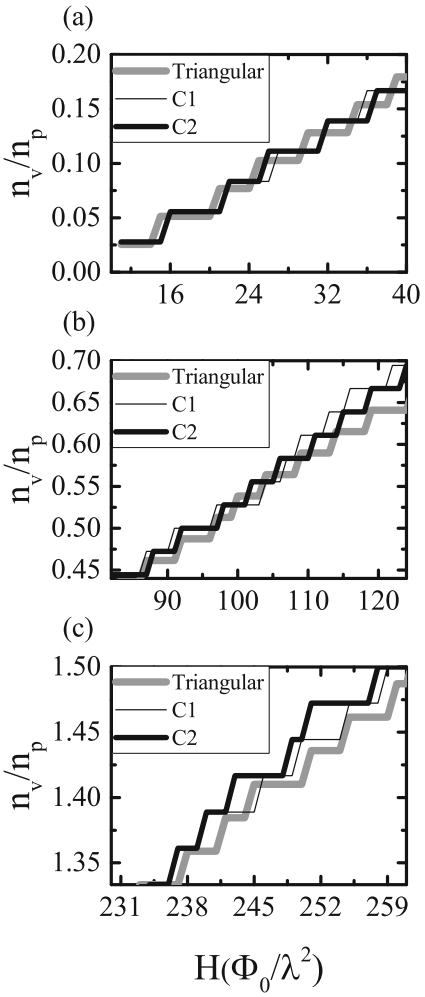

Fig. 3 The rate n_v/n_p for selected values of applied magnetic field H to show in greater detail the vortex nucleation shown in Fig. 2, for **a** low, **b** intermediate, and **c** high values of applied field. In **a**, the triangular lattice shows the lowest barrier for vortex penetration. In **b**, C1 is more favorable for vortex penetration. In **c**, C2 favors the penetration of vortices in the strip

However, there is still an open question: for a given number of pinning centers, how does their distribution influence a new nucleation. With this purpose, in Fig. 2, we show our results obtained for the vortex density as a function of the applied magnetic field in strips with triangular and conformal pinning arrays.

From Fig. 2, it is possible to see the monotonic increase, by steps, of the vortex density as a function of the magnetic field for all pinning landscapes, which is typical of finite size samples [76, 84, 88, 90, 95]. Moreover, it is necessary to notice that for each pinning array and given n_v/n_p value, the field for a new vortex penetration is different, as we can see in Fig. 3. In Fig. 3a, we can see that in the range of fields

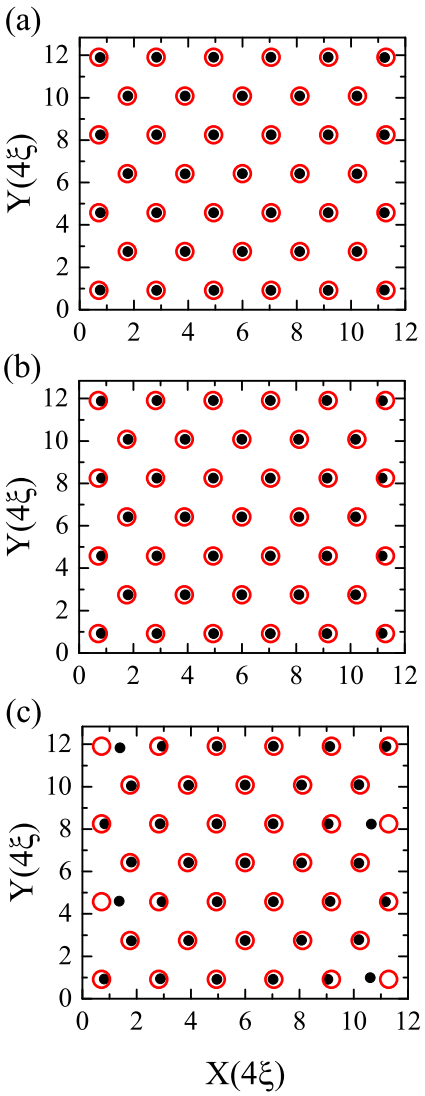

Fig. 4 Main simulation box, where the red open circles represent the triangular pinning array and the black dots the vortices for **a** $H = 168$, **b** $H = 172$, and **c** $H = 177$. As the applied magnetic field increases, vortices are dislocated towards the center of the sample destroying the commensurability. The pinning range used is $a_p = \xi$ and $C_p = 0.2C_v$. The lengths x and y are normalized in units of 4ξ

between $10 < H < 40$, for the triangular pinning array, the delay is smaller than for C1 and C2 arrays. However, panels b and c of Fig. 3 show that the vortex penetration delay is smaller for the conformal pinning array C1 in the range of fields $85 < H < 125$ and for C2 in the range $233 < H < 260$, respectively.

The triangular pinning array exhibits a shorter delay for lower magnetic fields because the pinning density is higher close to the edge of the strip when compared to the conformal arrays, as can be seen clearly in Fig. 1. The attractive interaction associated to the pinning centers close to the surface favors the penetration of vortices inside the strip. Besides, for low values of magnetic field, vortices stabilize close to the center of the strip, reducing the barrier for a new vortex penetration. In the range of fields $85 < H < 125$, the C1 array exhibits a smaller vortex penetration delay than the other arrays due to the low vortex density close to the edge of the strip, favoring the vortex penetration. For high values of field, the C2 array presents smaller delays for the same reason.

Another interesting characteristic observed in Fig. 2 is that the triangular array for $n_v/n_p = 1$ is stable in a wider range of fields than for other values of this ratio. In the range of fields where $n_v/n_p = 1$, the vortex lattice goes from an ordered and commensurate to a disordered and uncommensurate state, as the field is increased. In Fig. 4, it is possible to see the vortex lattice evolution as the magnetic field is increased.

In fact, this vortex lattice deformation is observed for all pinning lattices. As an example, in Fig. 5 is illustrated the case of C1 and C2 arrays at $n_v/n_p = 2/3$. As can be seen, the vortex lattice can change from ordered to disordered configuration (see Fig. 5a, b for C1) or vice versa (see Fig. 5c, d for C2). These deformations of the vortex lattice as a function of the applied field will directly influence the depinning forces of the system as we will see in the next section.

4 Critical Depinning Forces and Vortex Motion

The dynamical properties are obtained by numerical integration of the Langevin equations [see (1)] for several values of applied magnetic field H. As a result, we obtained the vortex positions for every time step t, which permits to evaluate the vortex average velocity V, the depinning forces, and the vortex trajectories along the strip. The results for the depinning forces, F_D, as a function of the applied magnetic field, H, are plotted in Fig. 6.

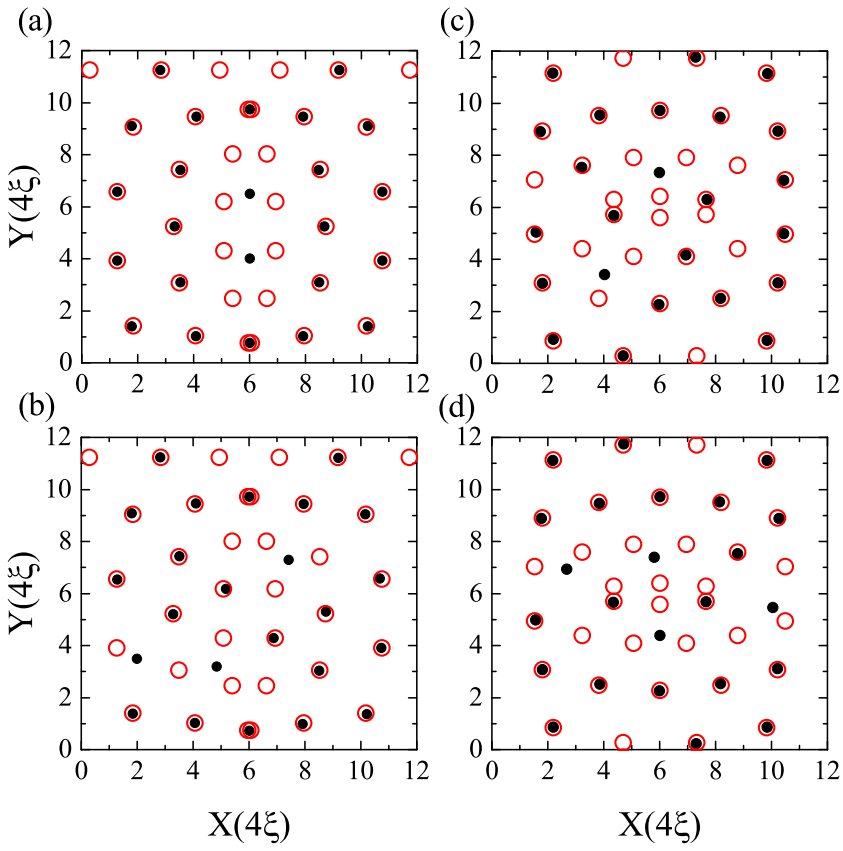

Fig. 5 Main simulation box, where the red open circles represent the pinning centers and the black dots the vortices for $n_v/n_p = 2/3$ at **a** $H = 116$ and **b** $H = 121$ for the C1 array, **c** $H = 119$ and **d** $H = 123$ for the C2 array. The pinning range used is $a_p = \xi$ and $C_p = 0.2C_v$. The lengths x and y are normalized in units of 4ξ

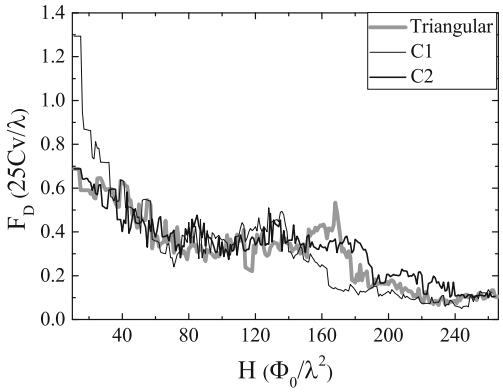

Fig. 6 Depinning forces F_D as a function of the applied magnetic field H for all pinning distributions studied in this work. The magnetic field H is in units of Φ_0/λ^2, and the force F_D in units $25C_v/\lambda$

As mentioned before, there is a commensurability effect for the triangular pinning array at $n_v/n_p = 1$ (see Fig. 4a) which results in a pronounced critical depinning force peak at $H = 168$ (see Fig. 6). This is the only peak that we can associate to commensurability effects in the superconducting strip. This result is different from what is observed in infinite superconducting films, where clear commensurability effects at submatching fields can be seen at $n_v/n_p = 1/4, 1/3, 1/2, 2/3$, and $3/4$ [33, 35, 36, 41]. In strips, the surface barrier prevents the commensurability force peaks at submatching fields by forcing vortices to stabilize in interstitial positions towards the center of the sample, lowering the pinning force.

In Fig. 6, is possible to see that the system exhibits fluctuations in the depinning forces. From Fig. 2, we can see that a given density of vortices remains stable between a range of fields. However, the vortex configuration deforms as the magnetic field is increased (see, for example, Figs. 4 and 5). The deformation in the vortex lattice induces variations in the pinning force and, as a consequence, provokes changes in the critical depinning forces. This behavior can be seen in detail in Fig. 7, where we show the magnification, for selected values of field, of Fig. 6. The

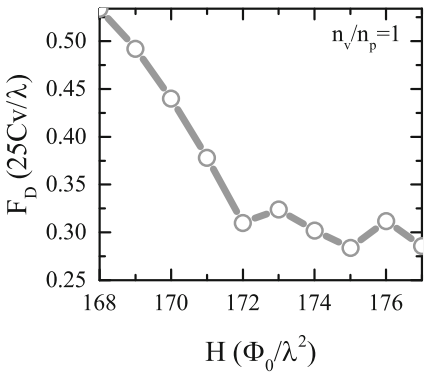

Fig. 7 Depinning forces F_D as a function of the applied magnetic field H for the triangular pinning array at $n_v/n_p = 1$

depinning forces are plotted as a function of the applied magnetic field for $n_v/n_p = 1$. In this case, for $H = 168$, the vortex lattice is fully commensurate and the depinning force is the highest. As the magnetic field is increased, the vortex lattice deforms destroying the commensurability (see Fig. 4c) and leading to a decrease in the depinning forces. For other values of n_v/n_p, the critical depinning forces may increase or decrease with the magnetic field depending on the particular vortex configurations, which explains the fluctuations in the critical forces.

The results observed for the conformal arrays (C1 and C2) show that there are no pronounced force peaks for any values of applied magnetic field. This is in agreement with observations of infinite superconducting films with conformal pinning distributions [56–59, 62, 63]. The main characteristic of this distribution is the stability of the depinning forces for a wide range of fields. In fact, we observe this characteristic for both arrays, where the depinning forces fluctuate, but in general, we observe the absence of critical depinning force peaks as the magnetic field is varied. In the range $0 < n_v/n_p < 1$, we observe that at low fields the depinning forces are higher for the C1 than the C2 array. This can be explained by the association of surface and pinning density effects. In strips with the absence of pinning centers, vortices usually stabilize close to the center of the strip, forming rows of vortices [76, 78]. In the C1 case, the pinning density is always higher at the center of the strip. Thus, the pinning is very effective for low values of field, where the vortex rows stabilize in the central region of the strip matching with the pinning lattice and enhancing the depinning forces. However, as the magnetic field increases, the vortex rows begin to stabilize in peripheric regions, where the pinning is reduced. As a consequence, the depinning forces decrease rapidly.

For values of $32 \geq H \geq 152$, C1 and C2 arrays exhibit similar behavior concerning to depinning forces. However, for $H > 152$, the C2 array is more efficient than C1 due to the formation of easy vortex flow channels in the C1 array. In previous simulations with infinite samples [57], it has been shown that the conformal distribution is very efficient to prevent the formation of channels of easy vortex flow, for several transport force angles. However, in our case, the size effects seem to favor the formation of these easy channels for the C1 array. In order to verify the formation of these easy channels in our superconducting strip, we analyze the vortex dynamical phases and trajectories for $n_v/n_p > 1$, where $H > 152$. First, we analyze the vortex motion in the C2 array for the case of $H = 205$, where $n_v/n_p = 1.14$. Figure 8 shows the vortex velocity, V_y, as a function of the transport force, F_y. As a result, it is possible to see that the system presents only one dynamical transition, from static to the moving phase, i.e. all vortices begin to move at the same time.

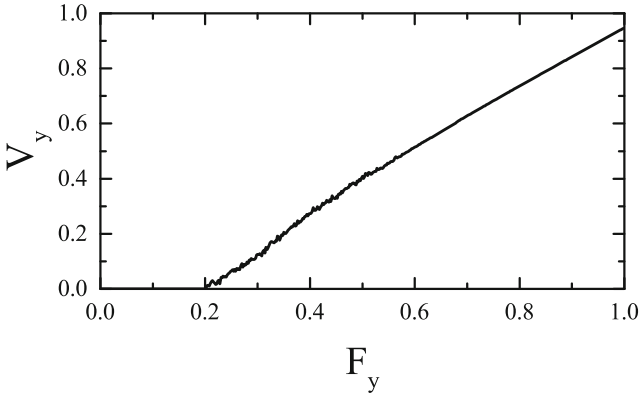

Fig. 8 Vortex velocity V_y as a function of the applied transport force F_y for the C2 array with $H = 205$, where $n_v/n_p = 1.14$

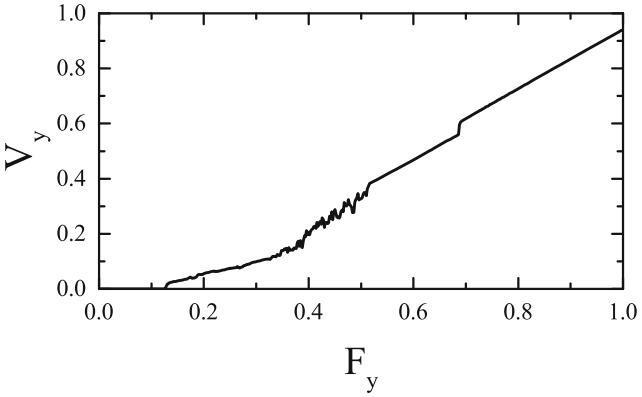

Fig. 10 Vortex velocity V_y as a function of the applied transport force F_y for the C1 array with $H = 200$, where $n_v/n_p = 1.11$

In Fig. 9, we plot the snapshots of the vortices for some transport force values. Figure 9a illustrates the static phase. When the transport force reaches its critical depinning value, all vortices depin at the same time and flow along the strip by tortuous channels with interconnectivity (see Fig. 9b). Due to the absence of weak spots, the C2 array is efficient to prevent easy vortex flow channels for high applied field values. As the transport force increases, vortices begin to form narrow channels without interconnectivity (see Fig. 9c).

The efficiency of the C1 array is especially reduced when $n_v/n_p > 1$, where vortices stabilize closer to the sample edge. In Fig. 10 is plotted the average vortex velocity, V_y, as a function of the transport force, F_y, for the case of $H = 200$ where $n_v/n_p = 1.11$. In Fig. 11, we show the vortex trajectories along the strip.

The vortex ground state (see Fig. 11a) remains static until reaching the critical depinning force, $F_D = 0.126$. Above the critical depinning force (see Fig. 11b), vortices close to the edge of the strip depin and flow in the direction

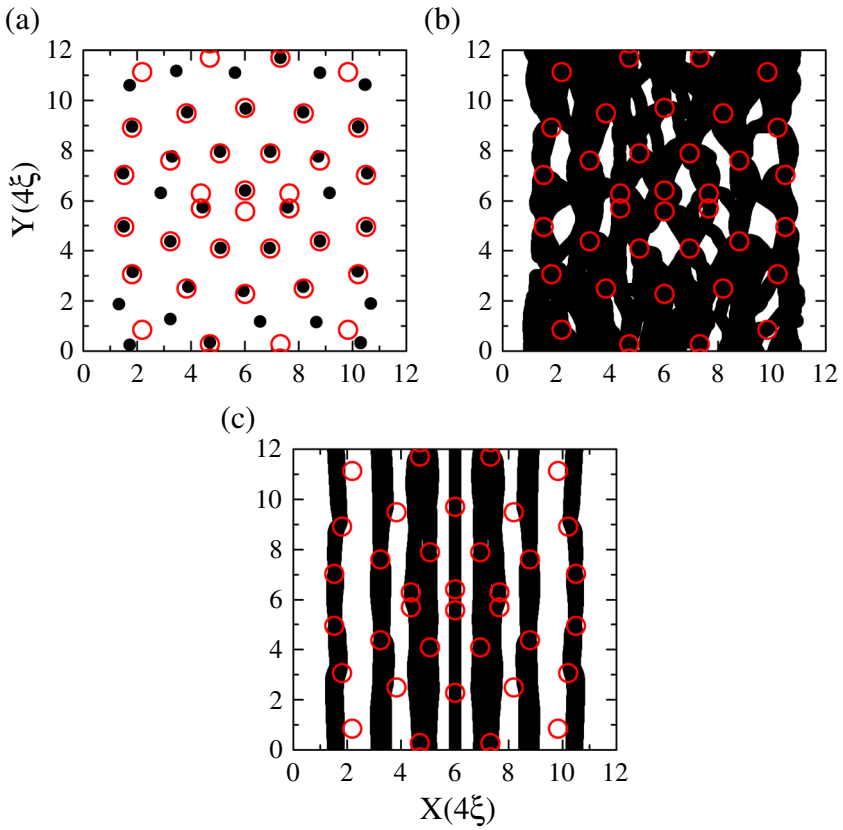

Fig. 9 Main simulation box, where the red open circles represent the C2 pinning array and the black dots the vortices for $H = 205$. In **a**, the applied force is $F_y = 0.196$, **b** $F_y = 0.288$, and **c** $F_y = 1.000$ In this case, all vortices depin at the same time and the formation of vortex channels occurs slowly as the transport force increases. The pinning range used is $a_p = \xi$ and $C_p = 0.2C_v$ The lengths x and y are normalized in units of 4ξ

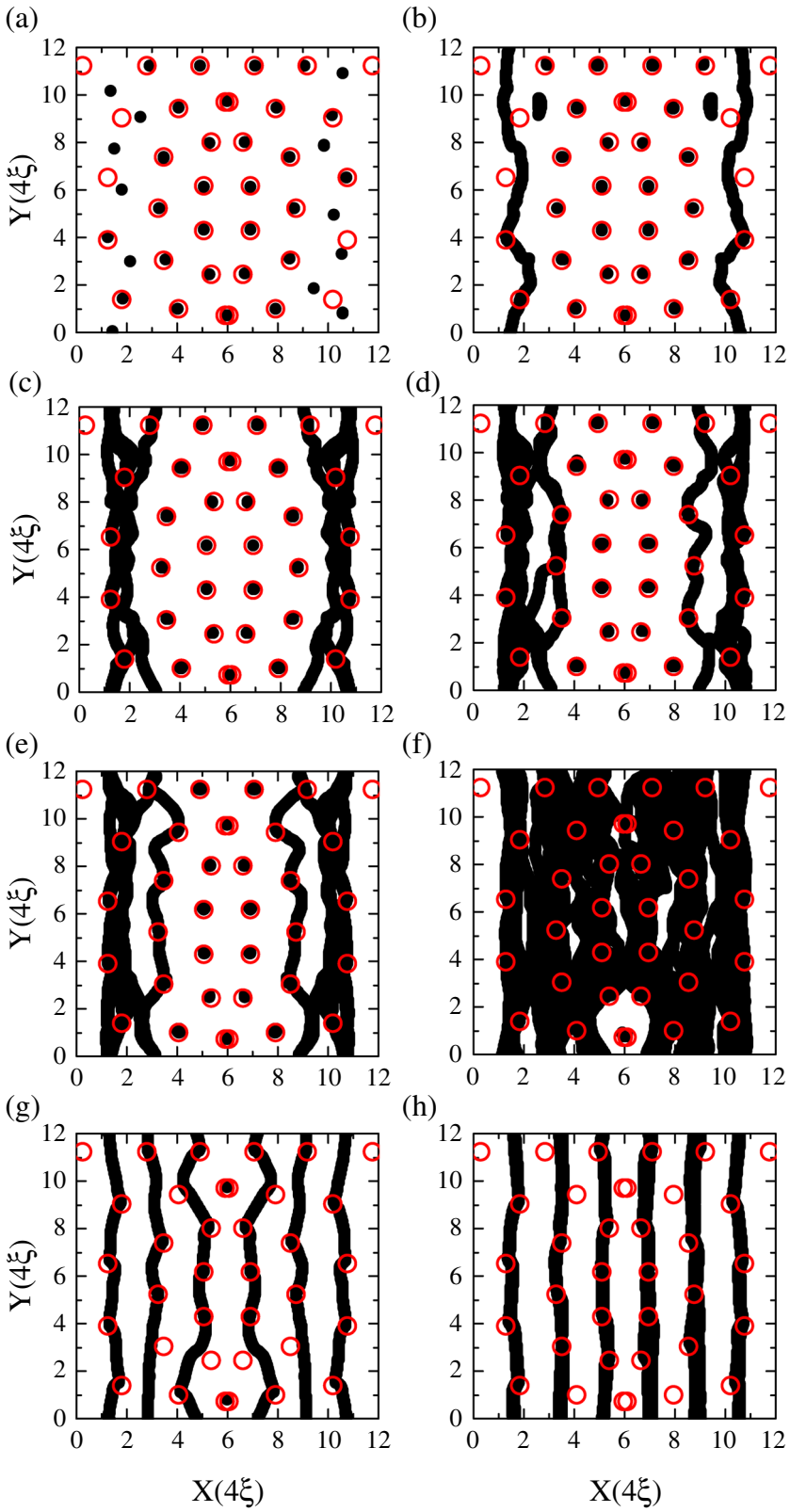

Fig. 11 Main simulation box, where the red open circles represent the C1 pinning array and the black dots the vortices for $H = 200$. In **a**, the applied force is $F_y = 0.100$, **b** $F_y = 0.130$ **c** $F_y = 0.182$, **d** $F_y = 0.194$, **e** $F_y = 0.318$, **f** $F_y = 0.450$, **g** $F_y = 0.700$, and **h** $F_y = 1.000$ As the transport force increases, vortices form channels from the edge of the sample to the center of the sample. The pinning range used is $a_p = \xi$ and $C_p = 0.2C_v$ The lengths x and y are normalized in units of 4ξ

of the transport force, forming a tortuous narrow channel. It is clear from Fig. 11a that there are weak spots close to the edge of the sample, which enables the formation of easy vortex flow channels. As the transport force is increased, at $F_y = 0.182$ (see Fig. 11c), more vortices depin resulting in curved tortuous vortex channels following the

pinning arches of the conformal array close to the edge. Note that the two internal pinning arches still maintain the vortices trapped. After further increasing of the drive, at $F_y = 0.194$ (see Fig. 11d), part of the vortices from the intermediary pinning arches depin in complex vortex trajectories. Above $F = 0.318$, more vortices depin from the intermediary arches (see Fig. 11e). When the transport force reaches $F_y = 0.334$, vortices from the central arches of the conformal lattice depin in a regime which shows several fluctuations in the velocity curve and disordered vortex lattice (see Figs. 10 and 11f). When the transport force reaches $F_y = 0.334$, the system reorders in narrow channels. However, two vortices are still trapped, each one to the almost overimposed pinning sites in the extremes of the central arches (see Fig. 11g). Above $F_y > 0.690$, vortices depin and the system goes to a regime where all vortices flow though the strip (see Fig. 11h). It can be seen in Fig. 11h that vortices flow following the arches of the conformal landscape. Thus, the C1 array is able to guide the vortex motion through the strip. A similar kind of guidance was observed in infinite superconducting bulks with conformal pinning by Ray et al., where vortices were more likely to move in regions with low pinning density [57].

The C1 array presents a higher density of pinning centers at the center of the strip, which enhances the pinning in that region and avoids the vortex movement. However, in regions next to the edge of the sample, the pinning is reduced giving rise to weak spots and vortices are more likely to move. We also observe that the depinning occurs via vortices in the same pinning arch, starting from arches close to the edge and moving to those close to the center.

5 Conclusions

In summary, we have shown the vortex behavior in type II superconducting strips with the presence of triangular and two kinds of conformal pinning arrays (C1 and C2) at zero temperature.

Our results show that in strips there is a monotonic increase, by steps, of the vortex density as a function of the applied magnetic field, in analogy with previous works in the absence of pinning centers [76, 78, 88–90, 95]. However, the pinning distribution in the sample influences the vortex nucleation. For the case of triangular arrays, it was observed that for low values of applied magnetic field, the vortex penetration delay is smaller than for C1 and C2 arrays. This is a consequence of the higher pinning density present close to the edge of the strip when compared to both conformal arrays. Besides, for low values of field, vortices stabilize in the central region of the strip, reducing the vortex-vortex repulsion. However, for intermediate values of magnetic field, the C1 array exhibits a smaller delay when compared to the other lattices. This may be understood by the low vortex density close to the edge of the strip when compared to other lattices, which enables the vortex penetration. For high field values, the C2 landscape exhibits smaller delays to vortex penetration for the same reason. We also show that for a given value of n_v/n_p, the vortex configuration may change due to surface effects. This change can go from ordered to a disordered lattice, or vice versa. As a consequence, these changes directly influence the depinning forces, resulting in fluctuations with the magnetic field.

Concerning to critical depinning forces, our results show that for the triangular pinning array, there is a clear commensurability effect at $n_v/n_p = 1$. However, that commensurability peak is not present in all the range of magnetic field where $n_v/n_p = 1$. The peak appears only for $H = 168$, where the vortex lattice is ordered and commensurate. As the magnetic field increases for the same value of n_v/n_p, the lattice deforms and the commensurability is lost, as can be seen in Fig. 4. However, this is the only pronounced depinning force peak that can be associated with commensurability in our calculations. This result is very different to that observed in infinite superconducting films with triangular pinning, where several matching and submatching features were found [33, 35, 36, 41]. This is a consequence of the surface barrier pushing vortices to stabilize in interstitial positions towards the center of the sample, destroying the commensurability. For C1 and C2 arrays, we observed fluctuations in the depinning forces, but a complete absence of pronounced force peaks for any values of magnetic fields, in agreement with observations for infinite samples [56–59, 62, 63]. Our results show that at low fields the C1 array is more efficient that C2, while at high fields C2 is more efficient than C1. The C1 array exhibits high pinning density in the central region of the strip, which matches the vortex lattice for low values of field and enhances the depinning forces. However, at high fields, vortices stabilize close to the edge of the strip, where the pinning density is lower. Hence, the depinning forces are greatly reduced as the magnetic field is increased. For the C2 case, at high field values, the gradient of pinning centers associated to the arching structure of the conformal landscape prevents the formation of easy vortex flow channels, enhancing the depinning forces.

In order to investigate the formation or not of easy vortex flow channels, we analyzed the vortex dynamics for both conformal arrays when $n_v/n_p > 1$. Our analysis shows that the depinning transition in the C2 array occurs with all vortices moving at the same time, indicating that there are no weak spots and the easy vortex channels were avoided. In contrast, we observed that in the C1 array there are weak spots close to the edge of the strip giving rise to easy vortex

flow channels, resulting in the depinning of the arch closer to the edge. Moreover, vortices flow following the pinning arch structures, which may be used as a guide for the vortex motion.

Funding Information N.P.V. and M.C. acknowledge Capes-Brazil for financial support. L.G.V. acknowledges the support from the Brazilian Government's Science Without Borders Programme (Grant: 206419/2014-7). This research was supported by the Center for Scientific Computing (NCC/GridUNESP) of the São Paulo State University (UNESP).

References

1. Abrikosov, A.: On the magnetic properties of superconductors of the second group. Sov. Phys. JETP. **5**, 1174–1182 (1957)
2. Tinkham, M. Introduction to Superconductivity, Second Edition. Dover Publications, Mineola, NY (2004)
3. Pool, R.: Superconductivity: is the party over? Science **244**, 914–916 (1989). https://doi.org/10.1126/science.244.4907.914
4. Pool, R.: Superconductivity: party time again. Science **246**, 1243–1243 (1989). https://doi.org/10.1126/science.246.4935.1243
5. Brandt, E.H.: Computer simulation of flux pinning in type-ii superconductors. Phys. Rev. Lett. **50**, 1599–1602 (1983). https://doi.org/10.1103/PhysRevLett.50.1599
6. Buzdin, A., Feinberg, D.: On the theory of electromagnetic pinning of vortices. Phys. C Supercond. **235**, 2755–2756 (1994). https://doi.org/10.1016/0921-4534(94)92598-4
7. Matsumoto, K., Mele, P.: Artificial pinning center technology to enhance vortex pinning in YBCO coated conductors. Supercond. Sci. Technol. **23**, 014001 (2010). https://doi.org/10.1088/0953-2048/23/1/014001
8. Morgan, D.J., Ketterson, J.B.: Asymmetric flux pinning in a regular array of magnetic dipoles. Phys. Rev. Lett. **80**, 3614–3617 (1998). https://doi.org/10.1103/PhysRevLett.80.3614
9. Reichhardt, C., Zimányi, G.T., Grønbech-Jensen, N.: Complex dynamical flow phases and pinning in superconductors with rectangular pinning arrays. Phys. Rev. B. **64**, 014501 (2001). https://doi.org/10.1103/PhysRevB.64.014501
10. Blatter, G., Feigel'man, M.V., Geshkenbein, V.B., Larkin, A.I., Vinokur, V.M.: Vortices in high-temperature superconductors. Rev. Mod. Phys. **66**, 1125–1388 (1994). https://doi.org/10.1103/RevModPhys.66.1125
11. Koshelev, A.E., Vinokur, V.M.: Dynamic melting of the vortex lattice. Phys. Rev. Lett. **73**, 3580–3583 (1994). https://doi.org/10.1103/PhysRevLett.73.3580
12. Grigorenko, A.N., Bending, S.J., Van Bael, M.J., Lange, M., Moshchalkov, V.V., Fangohr, H., de Groot, P.A.J.: Symmetry locking and commensurate vortex domain formation in periodic pinning arrays. Phys. Rev. Lett. **90**, 237001 (2003). https://doi.org/10.1103/PhysRevLett.90.237001
13. Martín, J.I., Vélez, M., Hoffmann, A., Schuller, I.K., Vicent, J.L.: Temperature dependence and mechanisms of vortex pinning by periodic arrays of Ni dots in Nb films. Phys. Rev. B. **62**, 9110–9116 (2000). https://doi.org/10.1103/PhysRevB.62.9110
14. Moshchalkov, V.V., Baert, M., Metlushko, V.V., Rosseel, E., Van Bael, M.J., Temst, K., Bruynseraede, Y., Jonckheere, R.: Pinning by an antidot lattice: the problem of the optimum antidot size. Phys. Rev. B. **57**, 3615–3622 (1998). https://doi.org/10.1103/PhysRevB.57.3615
15. Reichhardt, C., Olson, C.J., Nori, F.: Dynamic phases of vortices in superconductors with periodic pinning. Phys. Rev. Lett. **78**, 2648–2651 (1997). https://doi.org/10.1103/PhysRevLett.78.2648
16. Ren, Q.-B., Luo, M.-B.: Dynamics of two-dimensional vortex system in a strong square pinning array at the second matching field. Phys. Lett. A. **377**, 1966–1969 (2013). https://doi.org/10.1016/j.physleta.2013.05.045
17. Cuadra-Solís, P.-J., García-Santiago, A., Hernandez, J.M., Tejada, J., Vanacken, J., Moshchalkov, V.V.: Observation of commensurability effects in a patterned thin superconducting Pb film using microwave reflection spectrometry. Phys. Rev. B. **89**, 054517 (2014). https://doi.org/10.1103/PhysRevB.89.054517
18. Yetis, H.: Transport properties of the multiple vortices in superconductors with square pinning arrays. Eur. Phys. J. B. **88**. https://doi.org/10.1140/epjb/e2015-50474-2 (2015)
19. Reichhardt, C., Nori, F.: Phase locking, devil's staircases, Farey trees, and Arnold tongues in driven vortex lattices with periodic pinning. Phys. Rev. Lett. **82**, 414–417 (1999). https://doi.org/10.1103/PhysRevLett.82.414
20. Harada, K., Kamimura, O., Kasai, H., Matsuda, T., Tonomura, A., Moshchalkov, V.V.: Direct observation of vortex dynamics in superconducting films with regular arrays of defects. Science **274**, 1167–1170 (1996). https://doi.org/10.1126/science.274.5290.1167
21. Field, S.B., James, S.S., Barentine, J., Metlushko, V., Crabtree, G., Shtrikman, H., Ilic, B., Brueck, S.R.J.: Vortex configurations, matching, and domain structure in large arrays of artificial pinning centers. Phys. Rev. Lett. **88**, 067003 (2002). https://doi.org/10.1103/PhysRevLett.88.067003
22. Zhu, B.Y., Liu, M., Xing, D.Y., Zhao, B.R., Zhao, Z.X.: Moving vortex crystal induced by commensurability effects in a superconductor with periodic pinning array. Phys. C Supercond. **361**, 107–113 (2001). https://doi.org/10.1016/S0921-4534(01)00295-7
23. Chen, Q.H., Shi, D.Q., Li, W.X., Zhu, B.Y., Moshchalkov, V.V., Dou, S.X.: Configuration-induced vortex motion in type-II superconducting films with periodic magnetic dot arrays. Supercond. Sci. Technol. **27**, 065004 (2014). https://doi.org/10.1088/0953-2048/27/6/065004
24. Gutierrez, J., Silhanek, A.V., Van de Vondel, J., Gillijns, W., Moshchalkov, V.V.: Transition from turbulent to nearly laminar vortex flow in superconductors with periodic pinning. Phys. Rev. B. **80**, 140514 (2009). https://doi.org/10.1103/PhysRevB.80.140514
25. Hoffmann, A., Prieto, P., Schuller, I.K.: Periodic vortex pinning with magnetic and nonmagnetic dots: the influence of size. Phys. Rev. B. **61**, 6958–6965 (2000). https://doi.org/10.1103/PhysRevB.61.6958
26. Reichhardt, C., Grønbech-Jensen, N.: Collective multivortex states in periodic arrays of traps. Phys. Rev. Lett. **85**, 2372–2375 (2000). https://doi.org/10.1103/PhysRevLett.85.2372
27. Cuppens, J., Ataklti, G.W., Gillijns, W., de Vondel, J.V., Moshchalkov, V.V., Silhanek, A.V.: Vortex dynamics in a superconducting film with a Kagome and a honeycomb pinning landscape. J. Supercond. Nov. Magn. **24**, 7–11 (2011). https://doi.org/10.1007/s10948-010-0893-7
28. Xue, C., Ge, J.-Y., He, A., Zharinov, V.S., Moshchalkov, V.V., Zhou, Y.H., Silhanek, A.V., Van de Vondel, J.: Mapping degenerate vortex states in a Kagome lattice of elongated antidots via scanning Hall probe microscopy. Phys. Rev. B. **96**, 024510 (2017). https://doi.org/10.1103/PhysRevB.96.024510
29. Reichhardt, C., Reichhardt, C.J.O.: Vortex molecular crystal and vortex plastic crystal states in honeycomb and Kagom'e pinning arrays. Phys. Rev. B. **76**, 064523 (2007). https://doi.org/10.1103/PhysRevB.76.064523
30. Cao, R., Horng, L., Wu, T.C., Wu, J.C., Yang, T.J.: Temperature dependent pinning phenomenon in superconducting Nb films with triangular and honeycomb pinning arrays. J. Phys. Condens. Matter. **21**, 075705 (2009). https://doi.org/10.1088/0953-8984/21/7/075705

31. Cao, R., Wu, T.C., Kang, P.C., Wu, J.C., Yang, T.J., Horng, L.: Anisotropic pinning in Nb thin films with triangular pinning arrays. Solid State Commun. **143**, 171–175 (2007). https://doi.org/10.1016/j.ssc.2007.04.037
32. Laguna, M.F., Balseiro, C.A., Domínguez, D., Nori, F.: Vortex structure and dynamics in kagom'e and triangular pinning potentials. Phys. Rev. B. **64**, 104505 (2001). https://doi.org/10.1103/PhysRevB.64.104505
33. Vizarim, N.P., Carlone, M., Verga, L.G., Venegas, P.A.: Critical forces at fractional matching fields in superconducting thin films with triangular pinning lattice. Mater. Res. **20**, 899–903 (2017). https://doi.org/10.1590/1980-5373-mr-2016-0696
34. Sadovskyy, I.A., Wang, Y.L., Xiao, Z.-L., Kwok, W.-K., Glatz, A.: Effect of hexagonal patterned arrays and defect geometry on the critical current of superconducting films. Phys. Rev. B. **95**, 075303 (2017). https://doi.org/10.1103/PhysRevB.95.075303
35. Reichhardt, C., Grønbech-Jensen, N.: Critical currents and vortex states at fractional matching fields in superconductors with periodic pinning. Phys. Rev. B. **63**, 054510 (2001). https://doi.org/10.1103/PhysRevB.63.054510
36. Ooi, S., Mochiku, T., Hirata, K.: Fractional matching effect in single-crystal films of with antidot lattice. Phys. C Supercond. **469**, 1113–1115 (2009). https://doi.org/10.1016/j.physc.2009.05.206
37. Vizarim, N.P., Carlone, M., Verga, L.G., Venegas, P.A.: Commensurability effects in the critical forces of a superconducting film with kagomé pinning array at submatching fields. Eur. Phys. J. B. **90**, 169 (2017). https://doi.org/10.1140/epjb/e2017-80260-y
38. Reichhardt, C., Olson Reichhardt, C.J.: Transport anisotropy as a probe of the interstitial vortex state in superconductors with artificial pinning arrays. Phys. Rev. B. **79**, 134501 (2009). https://doi.org/10.1103/PhysRevB.79.134501
39. Berdiyorov, G.R., Milošević, M.V., Peeters, F.M.: Superconducting films with antidot arrays—novel behavior of the critical current. EPL Europhys. Lett. **74**, 493 (2006). https://doi.org/10.1209/epl/i2006-10013-1
40. Berdiyorov, G.R., Milošević, M.V., Peeters, F.M.: Vortex configurations and critical parameters in superconducting thin films containing antidot arrays: nonlinear Ginzburg-Landau theory. Phys. Rev. B. **74**, 174512 (2006). https://doi.org/10.1103/PhysRevB.74.174512
41. Bothner, D., Seidl, R., Misko, V.R., Kleiner, R., Koelle, D., Kemmler, M.: Unusual commensurability effects in quasiperiodic pinning arrays induced by local inhomogeneities of the pinning site density. Supercond. Sci. Technol. **27**, 065002 (2014). https://doi.org/10.1088/0953-2048/27/6/065002
42. Kemmler, M., Gürlich, C., Sterck, A., Pöhler, H., Neuhaus, M., Siegel, M., Kleiner, R., Koelle, D.: Commensurability effects in superconducting Nb films with quasiperiodic pinning arrays. Phys. Rev. Lett. **97**, 147003 (2006). https://doi.org/10.1103/PhysRevLett.97.147003
43. Misko, V.R., Savel'ev, S., Nori, F.: Critical currents in superconductors with quasiperiodic pinning arrays: one-dimensional chains and two-dimensional Penrose lattices. Phys. Rev. B. **74**, 024522 (2006). https://doi.org/10.1103/PhysRevB.74.024522
44. Misko, V., Savel'ev, S., Nori, F.: Critical currents in quasiperiodic pinning arrays: chains and penrose lattices. Phys. Rev. Lett. **95**, 177007 (2005). https://doi.org/10.1103/PhysRevLett.95.177007
45. Misko, V.R., Bothner, D., Kemmler, M., Kleiner, R., Koelle, D., Peeters, F.M., Nori, F.: Enhancing the critical current in quasiperiodic pinning arrays below and above the matching magnetic flux. Phys. Rev. B. **82**, 184512 (2010). https://doi.org/10.1103/PhysRevB.82.184512
46. Ray, D., Reichhardt, C., Reichhardt, C.J.O.: Vortex states in Archimedean tiling pinning arrays. Supercond. Sci. Technol. **27**, 075006 (2014). https://doi.org/10.1088/0953-2048/27/7/075006
47. Misko, V.R., Nori, F.: Magnetic flux pinning in superconductors with hyperbolic-tessellation arrays of pinning sites. Phys. Rev. B. **85**, 184506 (2012). https://doi.org/10.1103/PhysRevB.85.184506
48. Silhanek, A.V., Gillijns, W., Moshchalkov, V.V., Zhu, B.Y., Moonens, J., Leunissen, L.H.A.: Enhanced pinning and proliferation of matching effects in a superconducting film with a Penrose array of magnetic dots. Appl. Phys. Lett. **89**, 152507 (2006). https://doi.org/10.1063/1.2361172
49. Olson, C.J., Reichhardt, C.: Transverse depinning in strongly driven vortex lattices with disorder. Phys. Rev. B. **61**, R3811–R3814 (2000). https://doi.org/10.1103/PhysRevB.61.R3811
50. Olson, C.J., Reichhardt, C., Bhattacharya, S.: Critical depinning force and vortex lattice order in disordered superconductors. Phys. Rev. B. **64**, 024518 (2001). https://doi.org/10.1103/PhysRevB.64.024518
51. Olson, C.J., Reichhardt, C., Vinokur, V.M.: Hysteretic depinning and dynamical melting for magnetically interacting vortices in disordered layered superconductors. Phys. Rev. B. **64**, 140502 (2001). https://doi.org/10.1103/PhysRevB.64.140502
52. Ryu, S., Hellerqvist, M., Doniach, S., Kapitulnik, A., Stroud, D.: Dynamical phase transition in a driven disordered vortex lattice. Phys. Rev. Lett. **77**, 5114–5117 (1996). https://doi.org/10.1103/PhysRevLett.77.5114
53. Kolton, A.B., Exartier, R., Cugliandolo, L.F., Domínguez, D., Grønbech-Jensen, N.: Effective temperature in driven vortex lattices with random pinning. Phys. Rev. Lett. **89**, 227001 (2002). https://doi.org/10.1103/PhysRevLett.89.227001
54. Kolton, A.B., Domínguez, D., Grønbech-Jensen, N.: Hall Noise and transverse freezing in driven vortex lattices. Phys. Rev. Lett. **83**, 3061–3064 (1999). https://doi.org/10.1103/PhysRevLett.83.3061
55. Wu, T.C., Kang, P.C., Horng, L., Wu, J.C., Yang, T.J.: Anisotropic pinning effect on a Nb thin film with triangular arrays of pinning sites. J. Appl. Phys. **95**, 6696–6698 (2004). https://doi.org/10.1063/1.1690971
56. Ray, D., Olson Reichhardt, C.J., Jankó, B., Reichhardt, C.: Strongly enhanced pinning of magnetic vortices in type-II superconductors by conformal crystal arrays. Phys. Rev. Lett. **110**, 267001 (2013). https://doi.org/10.1103/PhysRevLett.110.267001
57. Ray, D., Reichhardt, C., Reichhardt, C.J.O.: Pinning, ordering, and dynamics of vortices in conformal crystal and gradient pinning arrays. Phys. Rev. B. **90**, 094502 (2014). https://doi.org/10.1103/PhysRevB.90.094502
58. Olson Reichhardt, C.J., Wang, Y.L., Xiao, Z.L., Kwok, W.K., Ray, D., Reichhardt, C., Jankó, B.: Pinning, flux diodes and ratchets for vortices interacting with conformal pinning arrays. Phys. C Supercond. Its Appl. **533**, 148–153 (2017). https://doi.org/10.1016/j.physc.2016.05.024
59. Ray, D., Reichhardt, C., Olson Reichhardt, C.J., Jankó, B.: Vortex transport and pinning in conformal pinning arrays. Phys. C Supercond. Its Appl. **503**, 123–127 (2014). https://doi.org/10.1016/j.physc.2014.04.038
60. Reichhardt, C., Reichhardt, C.J.O.: Transverse ac-driven and geometric ratchet effects for vortices in conformal crystal pinning arrays. Phys. Rev. B. **93**, 064508 (2016). https://doi.org/10.1103/PhysRevB.93.064508
61. Jing, Z., Yong, H., Zhou, Y.: Numerical simulation on the flux avalanche behaviors of microstructured superconducting thin films. J. Appl. Phys. **121**, 023902 (2017). https://doi.org/10.1063/1.4974000
62. Guénon, S., Rosen, Y.J., Basaran, A.C., Schuller, I.K.: Highly effective superconducting vortex pinning in conformal crystals.

Appl. Phys. Lett. **102**, 252602 (2013). https://doi.org/10.1063/1.4811413
63. Wang, Y.L., Latimer, M.L., Xiao, Z.L., Divan, R., Ocola, L.E., Crabtree, G.W., Kwok, W.K.: Enhancing the critical current of a superconducting film in a wide range of magnetic fields with a conformal array of nanoscale holes. Phys. Rev. B. **87**, 220501 (2013). https://doi.org/10.1103/PhysRevB.87.220501
64. Barba-Ortega, J., Sardella, E., Aguiar, J.A.: Superconducting boundary conditions for mesoscopic circular samples. Supercond. Sci. Technol. **24**, 015001 (2011). https://doi.org/10.1088/0953-2048/24/1/015001
65. Barba-Ortega, J., Sardella, E., Albino Aguiar, J., Peeters, F.M.: Non-conventional vortex configurations in a mesoscopic flat disk. Phys. C Supercond. **487**, 47–55 (2013). https://doi.org/10.1016/j.physc.2013.01.021
66. Barba-Ortega, J., Sardella, E., Albino Aguiar, J.: Temperature-dependent vortex matter in a superconducting mesoscopic circular sector. Phys. C Supercond. **470**, 1964–1967 (2010). https://doi.org/10.1016/j.physc.2010.08.008
67. Lisboa-Filho, P.N., Malvezzi, A.L., Sardella, E.: Minimum size for the occurrence of vortex matter in a square mesoscopic superconductor. Phys. B Condens. Matter. **403**, 1494–1496 (2008). https://doi.org/10.1016/j.physb.2007.10.247
68. Mel'nikov, A.S., Nefedov, I.M., Ryzhov, D.A., Shereshevskii, I.A., Vinokur, V.M., Vysheslavtsev, P.P.: Vortex states and magnetization curve of square mesoscopic superconductors. Phys. Rev. B. **65**, 140503 (2002). https://doi.org/10.1103/PhysRevB.65.140503
69. Sardella, E., Brandt, E.H.: Vortices in a mesoscopic superconducting disk of variable thickness. Supercond. Sci. Technol. **23**, 025015 (2010). https://doi.org/10.1088/0953-2048/23/2/025015
70. Sardella, E., Malvezzi, A.L., Lisboa-Filho, P.N., Ortiz, W.A.: Temperature-dependent vortex motion in a square mesoscopic superconducting cylinder: Ginzburg-landau calculations. Phys. Rev. B. **74**, 014512 (2006). https://doi.org/10.1103/PhysRevB.74.014512
71. Hernández, A.D., Baelus, B.J., Domínguez, D., Peeters, F.M.: Effects of thermal fluctuations on the magnetic behavior of mesoscopic superconductors. Phys. Rev. B. **71**, 214524 (2005). https://doi.org/10.1103/PhysRevB.71.214524
72. Berdiyorov, G., Harrabi, K., Maneval, J.P., Peeters, F.M.: Effect of pinning on the response of superconducting strips to an external pulsed current. Supercond. Sci. Technol. **28**, 025004 (2015). https://doi.org/10.1088/0953-2048/28/2/025004
73. Berdiyorov, G.R., Chao, X.H., Peeters, F.M., Wang, H.B., Moshchalkov, V.V., Zhu, B.Y.: Magnetoresistance oscillations in superconducting strips: a Ginzburg-Landau study. Phys. Rev. B. **86**, 224504 (2012). https://doi.org/10.1103/PhysRevB.86.224504
74. Berdiyorov, G.R., Elmurodov, A.K., Peeters, F.M., Vodolazov, D.Y.: Finite-size effect on the resistive state in a mesoscopic type-II superconducting stripe. Phys. Rev. B. **79**, 174506 (2009). https://doi.org/10.1103/PhysRevB.79.174506
75. Berdiyorov, G., Harrabi, K., Oktasendra, F., Gasmi, K., Mansour, A.I., Maneval, J.P., Peeters, F.M.: Dynamics of current-driven phase-slip centers in superconducting strips. Phys. Rev. B. **90**, 054506 (2014). https://doi.org/10.1103/PhysRevB.90.054506
76. Carneiro, G.: Equilibrium vortex-line configurations and critical currents in thin films under a parallel field. Phys. Rev. B. **57**, 6077–6083 (1998). https://doi.org/10.1103/PhysRevB.57.6077
77. Reis, J.D., Venegas, P.A., Mello, D.F., Cabrera, G.G.: Surface effects on moving vortices in superconducting stripes. Phys. C Supercond. **454**, 15–19 (2007). https://doi.org/10.1016/j.physc.2007.01.002
78. de Souza Silva, C.C., Cabral, L.R.E., Aguiar, J.A.: Flux penetration, matching effect, and hysteresis in homogeneous superconducting films. Phys. Rev. B. **63**, 134526 (2001). https://doi.org/10.1103/PhysRevB.63.134526
79. de Souza Silva, C.C., Cabral, L.R.E., Albino Aguiar, J.: Vortex configurations and metastability in mesoscopic superconductors. Phys. C Supercond. **404**, 11–17 (2004). https://doi.org/10.1016/j.physc.2003.11.060
80. Venegas, P.A.: Size effects in the magnetization of a superconducting wire. J. Appl. Phys. **85**, 6049 (1999). https://doi.org/10.1063/1.369078
81. Bean, C.P., Livingston, J.D.: Surface barrier in type-II superconductors. Phys. Rev. Lett. **12**, 14–16 (1964). https://doi.org/10.1103/PhysRevLett.12.14
82. de Souza Silva, C.C., Albino Aguiar, J.: Irreversible matching effects in homogeneous and layered superconducting films. Phys. C Supercond. **354**, 232–236 (2001). https://doi.org/10.1016/S0921-4534(01)00070-3
83. Benkraouda, M., Clem, J.R.: Magnetic hysteresis from the geometrical barrier in type-II superconducting strips. Phys. Rev. B. **53**, 5716–5726 (1996). https://doi.org/10.1103/PhysRevB.53.5716
84. Bronson, E., Gelfand, M.P., Field, S.B.: Equilibrium configurations of Pearl vortices in narrow strips. Phys. Rev. B. **73**, 144501 (2006). https://doi.org/10.1103/PhysRevB.73.144501
85. Kramer, R.B.G., Ataklti, G.W., Moshchalkov, V.V., Silhanek, A.V.: Direct visualization of the Campbell regime in superconducting stripes. Phys. Rev. B. **81**, 144508 (2010). https://doi.org/10.1103/PhysRevB.81.144508
86. Silva, C.C., de, S., Raes, B., Brisbois, J., Cabral, L.R.E., Silhanek, A.V., Van de Vondel, J., Moshchalkov, V.V.: Probing the low-frequency vortex dynamics in a nanostructured superconducting strip. Phys. Rev. B. **94**, 024516 (2016). https://doi.org/10.1103/PhysRevB.94.024516
87. Sánchez-Lotero, P., Domínguez, D., Aguiar, J.A.: Flux flow in current driven mesoscopic superconductors: size effects. Eur. Phys. J. B. **89**, 141 (2016). https://doi.org/10.1140/epjb/e2016-70047-1
88. Kuit, K.H., Kirtley, J.R., van der Veur, W., Molenaar, C.G., Roesthuis, F.J.G., Troeman, A.G.P., Clem, J.R., Hilgenkamp, H., Rogalla, H., Flokstra, J.: Vortex trapping and expulsion in thin-film $YBa_2Cu_3O_{7-\delta}$ strips. Phys. Rev. B. **77**, 134504 (2008). https://doi.org/10.1103/PhysRevB.77.134504
89. Palacios, J.J.: Vortex lattices in strong type-II superconducting two-dimensional strips. Phys. Rev. B. **57**, 10873–10876 (1998). https://doi.org/10.1103/PhysRevB.57.10873
90. Barba, J.J., Aguiar, J.A.: Bi-dimensional chain-like vortex structure in a mesoscopic superconductor. J. Phys. Conf. Ser. **150**, 052015 (2009). https://doi.org/10.1088/1742-6596/150/5/052015
91. Denisov, D.V., Shantsev, D.V., Galperin, Y.M., Choi, E.-M., Lee, H.-S., Lee, S.-I., Bobyl, A.V., Goa, P.E., Olsen, A.A.F., Johansen, T.H.: Onset of dendritic flux avalanches in superconducting films. Phys. Rev. Lett. **97**, 077002 (2006). https://doi.org/10.1103/PhysRevLett.97.077002
92. Mints, R.G., Rakhmanov, A.L.: Critical state stability in type-II superconductors and superconducting-normal-metal composites. Rev. Mod. Phys. **53**, 551–592 (1981). https://doi.org/10.1103/RevModPhys.53.551
93. Bardeen, J., Stephen, M.J.: Theory of the motion of vortices in superconductors. Phys. Rev. **140**, A1197–A1207 (1965). https://doi.org/10.1103/PhysRev.140.A1197
94. Tsallis, C., Stariolo, D.A.: Generalized simulated annealing. Phys. Stat. Mech. Its Appl. **233**, 395–406 (1996). https://doi.org/10.1016/S0378-4371(96)00271-3
95. Stan, G., Field, S.B., Martinis, J.M.: Critical field for complete vortex expulsion from narrow superconducting strips. Phys. Rev. Lett. **92**, 097003 (2004). https://doi.org/10.1103/PhysRevLett.92.097003